17

Mechanisms of Mutagenic DNA Nucleobase Damages and Their Chemical and Enzymatic Repairs Investigated by Quantum Chemical Methods

Eric A. C. Bushnell[1], Jorge Llano[2], Leif A. Eriksson[3] and James W. Gauld[1]
[1]*University of Windsor, Department of Chemistry and Biochemistry, Windsor, Ontario*
[2]*Grant MacEwan University, Department of Physical Sciences, Edmonton, Alberta*
[3]*School of Chemistry, National University of Ireland, Galway*
[1,2]*Canada*
[3]*Ireland*

1. Introduction

A cells genetic information, its 'blueprint of life', is contained within its DNA. This biologically important molecule, however, can be attacked by high–energy ionizing radiation and oxidizing agents resulting in a range of possible damage. For instance, nucleobases can undergo chemical modifications or degradation such as oxidation, deamination, alkylation or be cleaved from the sugar-phosphate backbone. (De Bont & van Larebeke 2004; Friedberg et al. 2004; Hecht 1999; Kamiya et al. 1998; Labet et al. 2008a; Lindahl 1993; Lysetska et al. 2002; Neeley & Essigmann 2006; Rydberg & Lindahl 1982; Taylor 1994; Wang 2008) Similarly, the deoxyribose sugar moieties may also undergo various chemical modifications. These events can lead further to the formation of DNA–DNA or DNA–protein cross–links or DNA–strand breaks. (Kumar & Sevilla 2010; Lipfert et al. 2004) Importantly, damage to DNA can significantly affect its replication and transcription. This can ultimately result in cell apoptosis or protein mutations and pathological diseases such as cancer. (Pages & Fuchs 2002)

Experimentally, there have been numerous detailed *in vivo* and *in vitro* investigations into the processes and pathways involved in the damage of DNA. (See, for instance, Kumar & Sevilla 2010; Mishina et al. 2006, Wetmore et al. 2001) Radiolysis experiments with photometric, electrochemical and electron paramagnetic resonance detection, enzymatic inhibition and mutagenesis studies have identified a large number of reaction intermediates and rate constants for many damage and repair processes. For more in-depth reviews of experimental investigations on DNA damage processes the reader is also directed to relevant chapters in this present book. Unfortunately, however, many uncertainties and questions still remain about DNA damage and repair.

Computational chemistry provides an alternate and also complementary approach for obtaining a deeper understanding of chemical processes. This is in part because it can not only be applied to systems that are amenable to experimental investigation but also to those

systems or reactions that may be too challenging or even impossible to study using such experimental techniques. Furthermore, it is nowadays possible to apply highly accurate and reliable computational methods to larger, more complete biochemical models. Thus, using such approaches one can not only reconcile theory with experiment but, for example, compare the feasibility of differing proposed reaction mechanisms or identify new pathways.

There have been numerous computational investigations on or related to DNA damage and repair. In this chapter the application of Computational Chemistry to the study of DNA damage and repair is illustrated through a review of a number of relevant computational investigations that we have performed. More specifically, we have applied high accuracy density functional theory (DFT)-based methods to the study of several important primary and secondary nucleobase damage pathways and repair mechanisms. The chapter is divided into sections, each of which focuses on select results concerning a damage and/or repair process involving either the nucleobase or phosphate components of DNA:

2. **Nucleobase oxidation via ionizing radiation**: describes primary redox damage in nucleobases. In particular, the Gibbs Free Energies of solution-phase electron (ET), proton (PT) and proton-coupled electron (PTET) transfers for all DNA bases are examined. In addition, the potential of alkylthiols to act as repair agents of such damage is considered.
3. **8-Oxopurine formation in purine, adenine and guanine**: focuses on secondary damage of purine nucleobases. Specifically, the mechanisms of $^{\bullet}OH$ attack leading to formation of 8–oxopurine derivatives are discussed as well as the Gibbs Free Energy changes of possible associated ET, PT and PTET processes.
4. **Deamination of oxidized cytosine**: examines the thermochemistry of several possible mechanisms by which oxidized cytosine, a pyrimidine nucleobase, may undergo deamination.
5. **Oxidation of serine phosphate: Implications for DNA**: investigates radicals formed from radiation–induced damage of serine phosphate.
6. **Oxidative repair of alkylated nucleobases: The catalytic mechanism of AlkB**: describes key results of our studies on the enzymatic mechanism of AlkB, a member of the family of α-ketoglutarate-Fe(II)-dependent dioxygenase enzymes that catalyse the oxidative repair of alkylated nucleobases.

1.1 Methods

For the detailed study of electronic properties of biochemical systems the current computational chemistry methods of choice for investigators are those of density functional theory (DFT). The principle reasons for this is that they inherently include electron correlation effects via their basis upon the electron density of the chemical system. Such effects are often important, for example, in accurately describing bond making and breaking processes, or weakly bound systems such as reaction transition structures. Furthermore, regardless of the number of electrons in the chemical system, the electron density is only ever a function of the three Cartesian coordinates. Thus, with such methods one can use larger and more complete chemical models consisting of 150 or more atoms. In addition, they are usually highly reliable and accurate.(See, for example, Llano 2010) For biochemical systems, the currently most widely used DFT functional is B3LYP,(Becke 1993a; Becke 1993b; Lee et al. 1988) and it has been used throughout this chapter.

Many biochemical processes occur within a polar environment, in particular an enzyme active site or aqueous medium. This can influence the properties and reactions of a biomolecule. Hence, it can be important to include such effects in the computational model. Each study described in this chapter has used a polarizable continuum (PCM)-based approach(Cammi & Tomasi 1995; Miertus et al. 1981) in the integral equation formulism (IEF).(Cances & Mennucci 1998; Cances et al. 1997; Mennucci et al. 1997) In this method the chemical system is effectively 'wrapped' in a density-fitting polar dielectric medium. Within this chapter a dielectric constant (ε) value of 4.0 has been used when modeling reactions within a protein active site, while the standard value for water at 298 K has been used for reactions modeled in aqueous environments. The specific computational details of each investigation are outlined in their respective section and in the appropriate article.
In order to determine relative free energies of reactions in which protons and electrons act as independent ions, it can be necessary to use 'fundamental values' such as the chemical potential of an electron or proton in a vacuum or aqueous solution under standard conditions. The values used in this chapter are given in **Table 1.** These have been obtained by means of a first principles quantum and statistical mechanics approach, the details of which are provided in a recent paper by Llano and Eriksson.(Llano & Eriksson 2002)

Quantity	eV	kcal mol^{-1}
$\mu_{0K}^{vac}(e^-)$	0.0	0.0
$\mu_{298K,1atm}^{\Theta,SHE}(e^-)$	–4.34 ± 0.02	–100.03 ± 0.5
$\mu_{298K,1atm}^{\Theta,aq}(e^-)$	–1.6638 ± 0.04	–38.37 ± 0.5
$\mu_{298K,1atm}^{\Theta,aq}(H^+)$	–11.6511 ± 0.02	–268.68 ± 0.5

Table 1. Chemical potentials of an electron in vacuum and an electron and proton in aqueous reference states.(Llano & Eriksson 2002).

2. Nucleobase oxidation via ionizing radiation

Ionizing radiation can potentially be absorbed by any of the three nucleotide components of DNA (i.e., phosphate, sugar or nucleobase) or its surrounding waters; also an essential part of DNA structure.(Kumar & Sevilla 2010) Primary damage of, for example, nucleobases, is caused by their direct absorption of radiation. Secondary damage (such as that described later in this chapter) can also occur, for instance, when the radiation is absorbed by the solvent, thus generating radicals or solvated electrons which then attack the nucleobase.(von Sonntag 1987; von Sonntag 1996)
Direct absorption (primary damage) can cause the formation of a radical-cationic base via the loss of an electron, i.e., generation of an electron hole. Due to the stacking of nucleobases within DNA charge transfer (transfer of the hole) can then occur along the strand. Consequently, this enables 'primary damage related' reactions to occur distant from the site of initial damage. The potential for charge transfer due to the π–orbital interactions between bases was proposed as early as 1962. (Eley & Spivey 1962) Alternatively, however, it may enable charge recombination to occur further along the chain. This is because radical-anionic bases can be formed by the capture of the free electrons, where the resulting damage to the nucleobase also constitutes primary damage. Guanine has the lowest ionization potential of

the four DNA nucleobases, followed by adenine.(Hush & Cheung 1975; Kumar & Sevilla 2010; Steenken & Jovanovic 1997; Yang et al. 2004) Consequently, they are in general oxidized to give their radical-cations while thymine and cytosine act as electron sinks and form their radical-anions. However, vice versa, in the transfer of electron holes guanine typically acts as a sink for DNA radiative oxidation.(Cadet et al. 2008; Kumar & Sevilla 2010) Reduction/oxidation of a nucleobase can significantly affect its properties. In particular, it has been shown that their oxidation greatly increases their acidity (lowers their pK_a).(Kumar & Sevilla 2010) Indeed, the formation of a radical base is often associated with proton transfer reactions that can lead to further nucleobase damage. However, as has also been noted, these same proton transfers can result in nucleobase repair.(Llano & Eriksson 2004b)

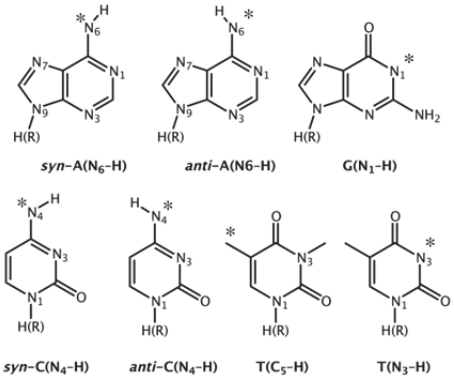

Fig. 1. Structures of the dehydrogenated nucleobases for both the cations and anions. The position of the missing hydrogen is marked by the asterisk.

Unfortunately, our understanding of these important electron- (ET) and proton-transfer (PT) reactions is incomplete.(Llano & Eriksson 2004a) This is not only due to the highly transient and reactive nature of key species involved, but also because experimental measurements of free energies for such processes can only be obtained indirectly.(Llano & Eriksson 2004a) Moreover, at times, the available experimental techniques (photoelectron spectroscopy, mass spectroscopy, pulse radiolysis and electrochemical techniques) appear to give contradictory results.(Seidel et al. 1996) Using computational methods we have investigated the processes involved in the oxidation and reduction of DNA nucleobases.(Llano & Eriksson 2004a) In particular, the nature of the ET process, the effect of PT on such processes, and vice versa, was examined using the chemical models shown in **Figure 1**.

All optimizations were performed at the B3LYP/6–31(+)G(d,p) level of theory; diffuse functions only being included for anionic species'. Harmonic vibrational frequencies and zero–point vibrational energies (ZPVE) were calculated at this same level of theory. Relative energies and absolute chemical potentials were then obtained via single point calculations at the IEF-PCM/B3LYP/6–311+G(2df,p) level of theory, in aqueous solvent, based on the above optimized structures with inclusion of the appropriate Gibbs corrections. In combination with the values listed in **Table 1**, the free energies for oxidation of the four neutral DNA bases and the corresponding anions was determined. Specifically, the free energies were calculated for the three different reference states used to define the absolute chemical potential of the electron: in vacuum, aqueous or the SHE reference state.

$B^{\bullet -}_{(aq)}$	⟶			$B_{(aq)}$	⟶			$B^{\bullet +}_{(aq)}$
	$-e^-_{(vac)}$	$-e^-_{(aq)}$	$-e^-_{(SHE)}$		$-e^-_{(vac)}$	$-e^-_{(aq)}$	$-e^-_{(SHE)}$	
$A^{\bullet -}$	40.7	2.3	–59.3 (–56.0)[a]	A	136.7	98.3	36.7 (32.7)[c]	$A^{\bullet +}$
$G^{\bullet -}$	37.9	–0.5	–62.1 (–63.2)[a]	G	125.9	87.5	25.9 (29.7)[c]	$G^{\bullet +}$
$T^{\bullet -}$	51.9	13.5	–48.1 (–25.6)[b]	T	145.2	106.8	45.2 (39.2)[c]	$T^{\bullet +}$
$C^{\bullet -}$	43.3	9.9	–51.7 (–25.8)[b]	C	147.6	109.2	47.6 (36.9)[c]	$C^{\bullet +}$

Table 2. Calculated (see text) standard free energies (in kcal mol^{-1}) of primary ionizations of the four nucleobases in aqueous solution. Experimental values are in parenthesis and taken from references: [a] (Seidel et al. 1996), [b] (Steenken et al. 1992), [c] (Steenken & Jovanovic 1997).

ET is a common process that occurs upon absorption of radiation by nucleobases. Using a first principles approach the free energy changes involved with such a process for all four DNA nucleobases were calculated and are shown in **Table 2**.(Llano & Eriksson 2002) It can be seen that the ionization of each of the anionic bases ($B^{\bullet -}_{(aq)}$) can be either endothermic or exothermic depending on the reference state of the electron. For example, in the vacuum or aqueous state the oxidation of the anionic bases is generally an endothermic process. The only exception occurs for guanine in the aqueous state in which the process is marginally exothermic (–0.5 kcal mol^{-1}). In contrast, in the case of the SHE reference state, oxidation of each base is markedly exothermic. For $A^{\bullet -}$ and $G^{\bullet -}$ the values calculated are in close agreement to those obtained experimentally.(Seidel et al. 1996; Steenken & Jovanovic 1997; Steenken et al. 1992) In contrast, those calculated for $C^{\bullet -}$ and $T^{\bullet -}$ are not in as good agreement, being almost twice the corresponding experimental values. However, the overall trends are consistent; the oxidation of $C^{\bullet -}$ or $T^{\bullet -}$ is thermodynamically less favorable than that of $A^{\bullet -}$ or $G^{\bullet -}$. Conversely, the reverse process, capture of a solvated electron by C or T (i.e., $C/T_{(aq)} + e^-_{(aq)} \rightarrow C/T^{\bullet -}_{(aq)}$) is thermodynamically preferred (–9.9 kcal mol^{-1} and –13.5 kcal mol^{-1}, respectively) compared to that involving A or G (–2.3 kcal mol^{-1} and 0.5 kcal mol^{-1}, respectively).

Oxidation of the neutral bases is calculated to be endothermic for each reference state of the electron (**Table 2**). The degree of endothermicity, however, depends on the reference state being most endothermic in vacuum and least for the SHE reference state. Unlike that observed for the radical anion bases, the SHE calculated values for the neutral bases are all in good agreement with experiment. The largest difference occurs for C and is now only 10.7 kcal mol^{-1} compared to the 25.9 kcal mol^{-1} difference for $C^{\bullet -}$, while the smallest difference (–3.8 kcal mol^{-1}) is observed for guanine. In addition, neutral G is calculated to have the lowest free energy of oxidation and is thus the easiest of the four DNA nucleobases to be ionized, in agreement with experimental observations.

The free energies associated with the loss of a proton from the resulting radical-cationic bases to solution were calculated and are given in **Table 3**. For $A/G^{\bullet +}$ the energy changes associated with deprotonations to form *syn*–A(N_6–H), *anti*–A(N_6–H), and G(N_1–H) were determined to be quite small at just –0.6, –0.7 and –0.3 kcal mol^{-1} respectively.(Llano & Eriksson 2004a) In contrast, the energy changes associated with deprotonation of $C/T^{\bullet +}$ to give *syn*–C(N_4–H) or *anti*–C(N4–H) and T(C_5–H) are larger at –5.2, –4.5 and –22.3 kcal mol^{-1}, respectively.(Llano & Eriksson 2004a) It is noted that T(C_5–H) has only been observed in the solid state and not in solution,(Steenken 1989) and thus will not be discussed herein. Unlike the other deprotonation processes, formation of T(N_3–H) was found to be endothermic and

Cationic Radical Base	ΔG (kcal mol^{-1})	Deprotonated Radical Base
$A^{\bullet+}$	–0.7 (≤ 1.4)[a]	*syn*–A(N_6–H),
$A^{\bullet+}$	–0.6 (≤ 1.4)[a]	*anti*–A(N_6–H)
$G^{\bullet+}$	–0.3 (5.3)[a]	G(N_1–H)
$T^{\bullet+}$	–22.3	T(C_5–H)
$T^{\bullet+}$	9.9 (4.9)[a]	T(N_3–H)
$C^{\bullet+}$	–5.2 (~5.4)[a]	*syn*–C(N_4–H),
$C^{\bullet+}$	–4.5 (~5.4)[a]	*anti*–C(N_4–H)

Table 3. Calculated (see text) standard Gibbs energies (in kcal mol^{-1}) of the decay of the radical cations. Experimental values included in parenthesis taken from references: [a] (Steenken 1989; Steenken 1992).

had the largest absolute free energy change (9.9 kcal mol^{-1}).(Llano & Eriksson 2004a) Thus, the loss of a proton in aqueous conditions is thermodynamically favorable for the radical-cationic bases except for proton loss from N_3—H in thymine. The unfavourable decay of $T^{\bullet+}$ via deprotonation of N_3–H suggests that the ion may have a long enough lifetime such that it may instead obtain an electron, a thermodynamically favourable process (**Table 2**). Thus, $T^{\bullet+}$ may instead preferably react to regenerate the neutral base T rather than decay.(Llano & Eriksson 2004a)

Having established an understanding of the energies associated with oxidation of the anionic and neutral bases, energy changes associated with possible repair mechanisms of this damage were then investigated. For the deprotonated neutral radical bases ($B(-H)^{\bullet}_{(aq)}$) regeneration can occur via three possible pathways: (i) ET followed by PT (**Table 4**); (ii) a proton-coupled electron transfer (PTET) (**Table 5**) or (iii) direct transfer of a hydrogen atom. From **Table 4** it can be seen that reduction of the deprotonated bases is exothermic under all reference states with the exception of $T(N_3–H)^{\bullet}$ in the SHE reference state. However, the energy change for protonating all of the reduced bases ($B(-H)^-_{(aq)}$) is favorable. Protonation of $G(N_1–H)^-$ has the smallest free energy change suggesting that the conjugate acid is relatively stronger than the other neutral bases. Importantly, the more acidic a molecule, the more powerful it is as a reducing agent. Thus, as G has the smallest energy cost of deprotonation of any of the DNA bases it is more likely to reduce the other bases and thereby act as an electron hole sink, as observed experimentally.

$B(-H)^{\bullet}_{(aq)}$	⟶			$B(-H)^-_{(aq)}$	⟶	$B_{(aq)}$
	$+e^-_{(vac)}$	$+e^-_{(aq)}$	$+e^-_{(SHE)}$		$+H^+_{(aq)}$	
syn–A(N_6–H)$^{\bullet}$	–113.2	–74.9	–13.2	*syn*–A(N_6–H)$^-$	–22.7 (≥ –19.1)[a]	A
anti–A(N_6–H)$^{\bullet}$	–113.9	–75.6	–13.9	*anti*–A(N_6–H)$^-$	–22.2 (≥ –19.1)[a]	A
G(N_1–H)$^{\bullet}$	–111.5	–73.2	–11.5	G(N_1–H)$^-$	–14.4 (–13.0)[a]	G
T(N_3–H)$^{\bullet}$	–72.3	–34.0	27.7	T(N_3–H)$^-$	–50.6	T
syn–C(N_4–H)$^{\bullet}$	–123.0	–84.6	–23.0	*syn*–C(N_4–H)$^-$	–19.4 (–17.7)[a]	C
anti–C(N_4–H)$^{\bullet}$	–123.4	–85.0	–23.4	*anti*–C(N_4–H)$^-$	–19.6 (–17.7)[a]	C

Table 4. Calculated (see text) standard Gibbs energies (in kcal mol^{-1}) of the regeneration of the nucleobases via a ET then PT process. Experimental values included in parenthesis taken from references: [a] (Steenken 1989; Steenken 1992).

Under alkaline conditions it is expected that ET would occur prior to PT, as seen in **Table 4**. However, under acidic conditions a PTET process may occur. The associated calculated energy values are given in **Table 5**. As can be seen, the free energy changes for ET are exothermic for all reference states when it occurs simultaneously with a PT. Importantly, the free energies associated with electron addition are decidedly more favorable in the case of a PTET process compared to that observed in the previous ET process (cf. **Table 4**).

$B(-H)^{\bullet}_{(aq)}$	⟶			$B_{(aq)}$
	$+e^-_{(vac)}$	$+e^-_{(aq)}$	$+e^-_{(SHE)}$	
syn–$A(N_6–H)^{\bullet}$	–136.0	–97.6	–36.0 (–46.8)[a]	A
anti–$A(N_6–H)^{\bullet}$	–136.1	–97.7	–36.1 (–46.8)[a]	A
$G(N_1–H)^{\bullet}$	–125.6	–87.3	–26.5 (–19.7)[a]	G
$T(N_3–H)^{\bullet}$	–155.1	–116.7	–55.1	T
syn–$C(N_4–H)^{\bullet}$	–142.4	–104.0	–42.4	C
anti–$C(N_4–H)^{\bullet}$	–143.0	–104.6	–43.0	C

Table 5. Calculated (see text) standard Gibbs energies of the regeneration of the nucleobases via a PTET process. Experimental values included in parenthesis taken from references: [a] (Steenken & Jovanovic 1997).

The aqueous state reduction of the neutral radical bases ($B(-H)^{\bullet}_{(aq)}$) by addition of $H^{\bullet}_{(aq)}$ was calculated to be exothermic for all DNA bases. More specifically, the free energy changes for reduction of *syn / anti*–$A(N_6–H)^{\bullet}$ and –$C(N_4–H)^{\bullet}$ are –85.0, –85.1, –91.4 and –92.0 kcal mol^{-1}, respectively while for $G(N_1–H)^{\bullet}$ and $T(N_3–H)^{\bullet}$ they are –74.6 and –104.1 kcal mol^{-1}, respectively. It is likely that this process is important under low pH conditions where the free protons would scavenge the hydrated electrons to yield $H^{\bullet}$. These free energy changes are less exothermic than those seen in the PTET process (cf. **Table 5**; $e^-_{(aq)}$ results). However, under acidic conditions the PTET and $H^{\bullet}$ processes would likely compete as they both react at diffusion-limited rates. Of all possible three reduction mechanisms for $B(-H)^{\bullet}$, PTET processes show the greatest change in free energy.

Deprotonated Radical Base	$\Delta_{ET}G^{\ominus}$	$\Delta_{PTET}G^{\ominus}$
syn–$A(N_6–H)^{\bullet}$	–5.1	–13.5
anti–$A(N_6–H)^{\bullet}$	–5.8	–13.6
$G(N_1–H)^{\bullet}$	–3.4	–3.1
$T(N_3–H)^{\bullet}$	–32.6	–32.6
syn–$C(N_4–H)^{\bullet}$	–14.9	–19.9
anti–$C(N_4–H)^{\bullet}$	–15.3	–20.5

Table 6. Calculated (see text) standard Gibbs energies (in kcal mol^{-1}) of the regeneration of the nucleobases by methylthiol. $\Delta_{ET}G^{\ominus}$ is the free energy change for $B(-H)^{\bullet}_{(aq)} + MeS^-_{(aq)} = B(-H)^-_{(aq)} + MeS^{\bullet}_{(aq)}$ while $\Delta_{PTET}G^{\ominus}$ is the free energy change for $B(-H)^{\bullet}_{(aq)} + MeSH_{(aq)} = B_{(aq)} + MeS^{\bullet}_{(aq)}$.

Clearly, the possible processes by which the neutral bases may be regenerated are inherently favorable regardless of whether the electrons originate from vacuum, dilute aqueous

solutions or SHE reference states. However, they still require that there be a suitable reductant. It has been noted that in solution a free thiol could be a likely reductant for transfer of a H• to a radical-cationic DNA base, thereby repairing the lesion.(von Sonntag 1987; von Sonntag 1996). Hence, the applicability of thiols to act as such a reductant was also investigated. It should be noted that although the process of repairing the nucleobase can occur via enzymatic or other chemical processes, only the latter involving methylthiol is discussed here. The calculated free energy costs associated with regeneration of the deprotonated radical bases by methylthiol (CH_3SH) are given in **Table 6**.

Two possible reduction pathways exist:

i. $B(-H)^{\bullet}_{(aq)} + MeS^-_{(aq)} \rightarrow B(-H)^-_{(aq)} + MeS^{\bullet}_{(aq)}$
ii. $B(-H)^{\bullet}_{(aq)} + MeSH_{(aq)} \rightarrow B_{(aq)} + MeS^{\bullet}_{(aq)}$

Pathway i most likely only occurs under basic conditions. However, as can be seen from **Table 6**, for *syn*– / *anti*–$A(N_6–H)^{\bullet}$ and –$C(N_4–H)^{\bullet}$ an initial loss of the –SH proton markedly lowers the reductive ability of the thiol. That is, the overall free energy change associated with regeneration of the nucleobases is reduced, i.e., $\Delta_{ET}G^{\ominus}$ is less exothermic than $\Delta_{PTET}G^{\ominus}$. However, for $G(N_1–H)^{\bullet}$ and $T(N_3–H)^{\bullet}$ the free energy changes are quite close for both possible regeneration pathways. The markedly larger values of $\Delta_{PTET}G^{\ominus}$ compared to $\Delta_{ET}G^{\ominus}$ for all adenine and cytosine species considered suggests that PTET is the favoured process at any pH for these nucleobases. However, the negligible difference observed for guanine and thymine suggest that the preferred path will depend on the reaction conditions, e.g., pH. Importantly, regardless of the preferred pathway the calculated free energies indicate they are both favorable, exothermic processes.

3. 8-Oxopurine formation in purine, adenine and guanine

A major type of secondary DNA damage is that caused by the attack of hydroxyl radicals.(Llano & Eriksson 2004a; von Sonntag 1987; von Sonntag 1996) Such radicals can be formed when metals or hydrogen peroxide are present.(Burrows & Muller 1998) In addition, however, the absorption of radiation by water can lead to not only the formation of solvated electrons but also of reactive oxygen species such as •OH. Furthermore, related modifications of nucleobases can occur via the reaction of their radical cation with water. For instance, reaction of $G^{\bullet+}$ with H_2O has been suggested to be an important alternative pathway in DNA modification.(Candeias & Steenken 2000) Unfortunately, due to the high reactivity of these radicals where the rates of reaction are typically diffusion controlled,(Llano & Eriksson 2004a) it is impossible for radical scavengers to prevent them from damaging DNA. It has been suggested that approximately half of the damage done by •OH occurs at the nucleobases. In the purine bases the hydroxyl has been observed to attack at their double bonds to form the C_4, C_5 and C_8 adducts with the latter (i.e., $\mathbf{B8OH^{\bullet}_{(aq)}}$) being the major product of oxidation and radiolysis.(Hagen 1986; Hatahet 1998; Kasai et al. 1986; Llano & Eriksson 2004b; Teoule 1987)

The subsequent oxidation of $\mathbf{B8OH^{\bullet}_{(aq)}}$ to give $\mathbf{8–OHB_{(aq)}}$ may occur via either of the two pathways shown in **Figure 2**: (i) a PT followed by an ET(Cullis et al. 1996) or (ii) a PTET mechanism(Candeias & Steenken 2000). The resulting common $\mathbf{8–OHB_{(aq)}}$ product of both pathways can then undergo tautomerization to yield the corresponding 8–oxo derivative ($\mathbf{8–oxoB_{(aq)}}$). It is noted that the barrier for tautomerization of 8–hydroxy–purine ($\mathbf{8–OHPu_{(aq)}}$) has been calculated to be quite low at only 7.0 kcal mol^{-1} with the keto form ($\mathbf{8–oxoPu_{(aq)}}$) being favoured over the enol form by 10.6 kcal mol^{-1}. (Llano & Eriksson 2004b)

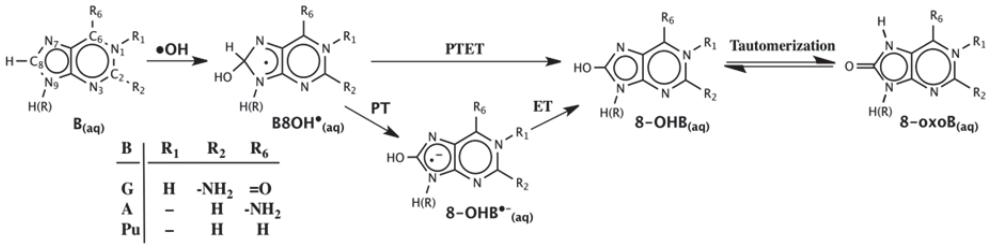

Fig. 2. Two proposed pathways for •OH attack at the C8 position of a purine base and subsequent oxidation to generate the 8-oxo purine derivative.

The **8–oxoG/A** products are in fact major stable DNA purine oxidation products produced via the radiolysis of water.(Hagen 1986; Hatahet 1998; Kasai et al. 1986; Teoule 1987) However, it is been observed that the adenine derivative (**8-oxoA**) is formed only about one–third of the time compared to the guanine derivative (**8-oxoG**).(Burrows & Muller 1998; Llano & Eriksson 2004b) Importantly, however, the formation of either **8–oxoB** species promotes the formation of mutagenic lesions that can cause mispairings resulting in G:C and T:A transversions.(Cheng et al. 1992; Cullis et al. 1996; Llano & Eriksson 2004b; Newcomb 1998; Pavlov et al. 1994) Such lesions are in fact caused by the further oxidation of **8–oxoB** to their corresponding **8–oxoB•(–H7)** derivatives. Moreover, it has been shown that depending on the reaction conditions both spiroiminodi- and guanidino-hydantoin are also major products formed by further oxidation of **8-oxoG**.(Munk et al. 2008) It has been suggested that these further reactions occur because the **8–oxoB** species' have lower ionization potentials than any other native base.(Cadet & Vigny 1990; Chatgilialoglu et al. 2000) Hence, they could act as a trap for a migrating electron hole.(Sponer et al. 2004; Yao et al. 2005) Unfortunately, however, despite detailed experimental study, the exact route by which such species' (**8-oxoB** and **8–oxoB•(–H7)**) may be formed remains unclear.(Llano & Eriksson 2004b)

We performed a computational investigation on the processes by which **8–OHB$_{(aq)}$** may be formed for purine, adenine and guanine.(Llano & Eriksson 2004b) In addition, the subsequent oxidations by which **8–oxoB** and **8–oxoB•(–H7)** may be formed were also examined using a first principles approach.(Llano & Eriksson 2002) Optimized structures, harmonic vibrational frequencies and ZPVEs were calculated at the B3LYP/6–31(+)G(d,p) level theory; diffuse functions only being included for anionic species'. Relative Gibbs Free energies were obtained by performing single point calculations at the IEF–PCM/B3LYP/6–311+G(2df,p) level of theory, in aqueous solvent, based on the above structures with inclusion of the appropriate Gibbs corrections.

Attack of •OH at the C_8 position in purine, adenine or guanine results in formation of the corresponding radical hydroxylated intermediates **B8OH•** (**Figure 3**). Notably, they are stabilized relative to the isolated reactants by –13.4, –14.9 and –15.8 kcal mol^{-1} for purine, adenine and guanine respectively.

The oxidation of **B8OH•$_{(aq)}$** may then be initiated via PT from its –C_8—H moiety (**Figure 3**). This step, resulting in formation of the corresponding radical-anionic derivatives **8–OHB•–$_{(aq)}$** was calculated to be significantly endothermic for all three purine bases considered with a minimum free energy cost of ~28 kcal mol^{-1}. Notably, the largest costs of 35.4 and 47.4 kcal mol^{-1} are observed for adenine and guanine, respectively. This suggests that a strong base is

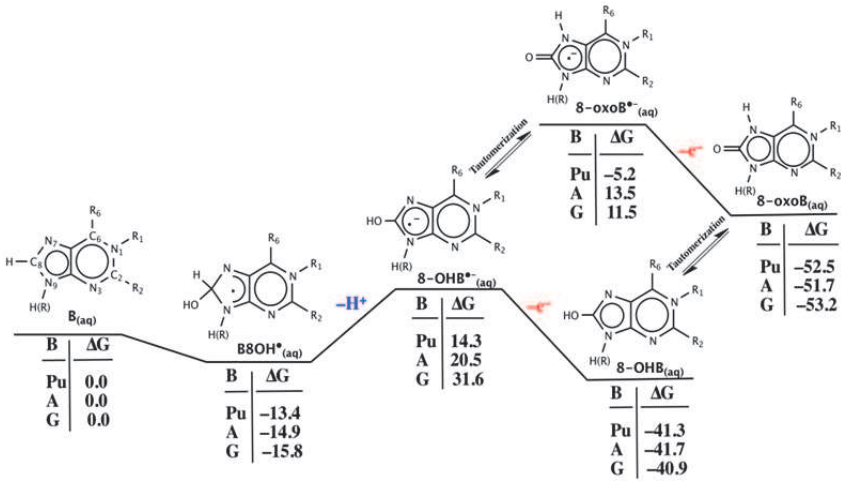

Fig. 3. Calculated (see text) standard Gibbs energies (kcal mol^{-1}) for PT initiated oxidation of **B8OH$^{\bullet}$.**

required for deprotonation of C_8 in **B8OH$^{\bullet}_{(aq)}$** and is unlikely to occur under neutral or acidic conditions. The resulting **8–OHB$^{\bullet-}_{(aq)}$** ions can then either oxidize further via loss of an electron to give **8–OHB$_{(aq)}$** or tautomerize to give **8–oxoB$^{\bullet-}_{(aq)}$**. As can be seen in **Figure 3**, both possible processes are thermodynamically preferred. Importantly, however, these latter two species can subsequently undergo tautomerization and electron loss, respectively to give the same **8–oxoB$_{(aq)}$** product species. The barriers for tautomerization of the radical-anionic (**8–OHPu$^{\bullet-}_{(aq)}$**) and neutral purine (**8–OHPu$_{(aq)}$**) are both low at just 5.2 and 7.1 kcal mol^{-1}, respectively. (Llano & Eriksson 2004b) Thus, the choice of pathway from **8–OHB$^{\bullet-}_{(aq)}$** to **8–oxoB$_{(aq)}$** may in fact be controlled by the thermodynamics of the loss of an electron. From **Figure 3** it can be seen that for purine and guanine the largest decreases in free energy observed for electron loss along either of these two paths occurs for the oxidation of the enol radical anion **8–OHB$^{\bullet-}_{(aq)}$** to give **8–OHB$_{(aq)}$** with decreases of 55.6 and 72.5 kcal mol^{-1} respectively. In contrast, for adenine the largest decrease (65.2 kcal mol^{-1}) is observed for loss of an electron from the keto radical anion **8–oxoB$^{\bullet-}_{(aq)}$** to give **8–oxoB$_{(aq)}$**. Thus for purine and guanine it is likely that formation of **8–oxoB$_{(aq)}$** occurs via tautomerization of **8–OHB$_{(aq)}$**, while for adenine it involves oxidation of **8–oxoB$^{\bullet-}_{(aq)}$**.

As shown in **Figure 4**, oxidation of **B8OH$^{\bullet}_{(aq)}$** may alternatively be initiated by ET, giving rise to **B8OH$^{+}_{(aq)}$** ions. Similar to that observed for an initial PT from **B8OH$^{\bullet}_{(aq)}$** (cf. **Figure 3**), this process is also found to be endothermic for all three purine nucleobases. However, with the exception of purine, the energy costs incurred are now significantly less. Indeed, for **A/G8OH$^{\bullet}_{(aq)}$** ET is thermodynamically preferred to PT by 24.1 and 47.2 kcal mol^{-1} respectively. It is further noted that for guanine, the reactant **G8OH$^{\bullet}_{(aq)}$** is essentially thermoneutral with the **G8OH$^{+}_{(aq)}$** intermediate. Furthermore, the subsequent PT from **B8OH$^{+}_{(aq)}$** to give **8–OHB$_{(aq)}$** is highly exothermic for all bases by 57.1, 45.3 and 25.3 kcal mol^{-1} for purine, adenine and guanine, respectively. This is in contrast to the highly endothermic initial PT observed in **B8OH$^{\bullet}_{(aq)}$** (cf. **Figure 3**). For the ET initiated oxidation pathway tautomerization can only happen once PT has occurred, that is, once **8–OHB$_{(aq)}$** has been formed. This rearrangement, which results directly in formation of **8–oxoB$_{(aq)}$**, is

exothermic for all bases considered by 10.0 – 12.3 kcal mol^{-1}. It should be noted that in addition to the possible ET and PT initiated processes, a PTET (i.e., the concerted loss of electron and proton) process may also occur. However, the overall free energy change for formation of **8–OHB** via this alternate path is –27.9, –26.8 and –25.1 kcal mol^{-1} relative to **B8OH$^{\bullet}$$_{(aq)}$** for purine, adenine and guanine, respectively.

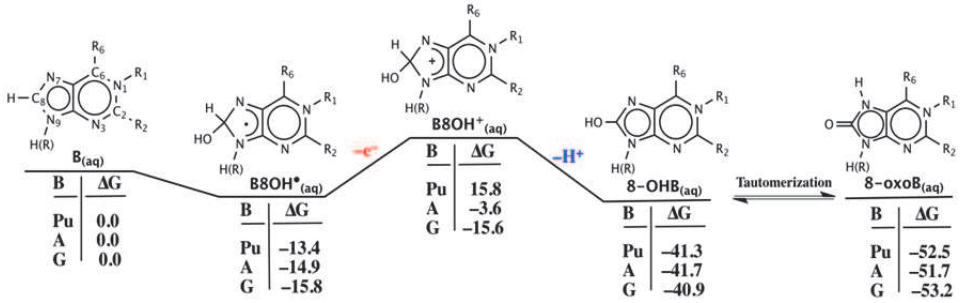

Fig. 4. Calculated (see text) standard Gibbs energies (kcal mol^{-1}) for the ET initiated oxidation pathway in **B8OH$^{\bullet}$**.

The formation of **8–oxoB$^{\bullet}$(–H7)$_{(aq)}$** can potentially be achieved by further oxidation of the neutral tautomers **8–oxoB$_{(aq)}$** and **8–OHB$_{(aq)}$**, initiated by loss of an electron (**Figure 5**). For both species', however, this ET process is endothermic. For purine and adenine the lowest associated energy costs (46.1 and 30.5 kcal mol^{-1} respectively) are incurred for ET from **8–oxoB$_{(aq)}$** while for guanine it is incurred from **8–OHB$_{(aq)}$** with a cost of 20.1 kcal mol^{-1}. Notably, for both **8–oxoB$_{(aq)}$** and **8–OHB$_{(aq)}$** the loss of an electron from the guanine-derivative (**8–oxoG$_{(aq)}$** and **8–OHG$_{(aq)}$**) is preferred to that from the corresponding adenine or purine-derivatives. Regardless, however, a suitable oxidant is required in order to oxidize either **8–oxoB$_{(aq)}$** or **8–OHB$_{(aq)}$**. The barriers for tautomerization for both the neutral **8–oxoB$_{(aq)}$/8–OHB$_{(aq)}$** and radical-cationic **8–OHB$^{\bullet+}$$_{(aq)}$/8–oxoB$^{\bullet+}$$_{(aq)}$** species' are quite low at

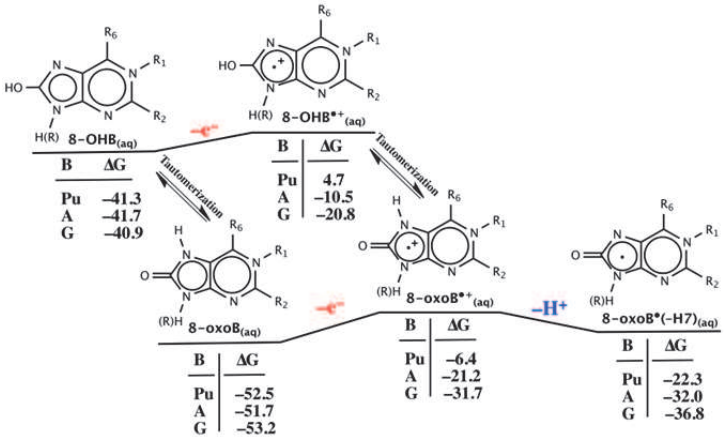

Fig. 5. Calculated (see text) standard Gibbs energies (kcal mol^{-1}) for oxidation of **8–OHB** and **8–oxoB.**

just 7.0 and 9.2 kcal mol^{-1}, respectively.(Llano & Eriksson 2004b) Thus, once formed, such species are expected to be able to easily interconvert between their enol and keto forms with equilibrium favouring the latter. However, once the **8–oxoB$^{\bullet+}_{(aq)}$** species is formed, loss of a proton (H^+) from N7 to give **8–oxoB$^{\bullet}$(–H7)$_{(aq)}$** is exothermic for all bases (**Figure 5**). Notably, **8–oxoG$^{\bullet}$(–H7)$_{(aq)}$** is calculated to lie 4.8 kcal mol^{-1} lower in energy than the corresponding adenine derivative **8–oxoA$^{\bullet}$(–H7)$_{(aq)}$** and may thus help explain the preference of its formation over that of **8–oxoA**.

4. Deamination of oxidized cytosine

In addition to damage by ionizing radiation it has been found that nucleobases are susceptible to oxidation by one–electron oxidants, e.g., nitrosoperoxycarbonate present during inflammatory processes.(Cadet et al. 2006; Lee et al. 2007) The purine base guanine, despite having the lowest ionization potential, is not the sole target for oxidants. In particular it has been observed that the pyrimidine bases are also susceptible to oxidation.(Decarroz et al. 1986; Douki & Cadet 1999; Wagner et al. 1990) Importantly, this oxidation leads to degradation via two possible competing pathways that are initiated by deprotonation of: (i) the methylene carbon of the sugar moiety (C_1') attached to the pyrimidine nitrogen (N_1) or (ii) the exocyclic amine attached to C_4 of the ring. Notably, the latter path has been suggested to lead to hydrolytic deamination of the pyrimidine ring.(Decarroz et al. 1987)

Previous computational investigations have investigated the deamination of non-oxidized cytosine, in particular via the attack of water or an hydroxyl anion (-OH) at its C_4 centre and via NO$^{\bullet}$ attack at N_4.(Almatarneh et al. 2006; Labet et al. 2009) While the lowest barrier was obtained for the nucleophilic attack of OH^- at C_4, the calculated value was 9.6 kcal mol^{-1} higher than that obtained experimentally. However, the susceptibility of cytosine to one–electron oxidation suggests that possible mechanisms for deamination of C$^{\bullet+}$ should also be taken into consideration. The importance of considering such reactions is further underlined by the fact that the product of oxidation and deamination of cytosine is the highly mutagenic uracil residue.

We used computational chemistry methods to investigate the deamination of cytosine via the oxidized cytosine intermediate C$^{\bullet+}$ and via a deprotonated cytosine. Optimized structures and their corresponding harmonic vibrational frequencies were obtained at the IEF–PCM/B3LYP/6–311G(d,p) level of theory in aqueous solvent. Relative free energies were obtained at the same level of theory with inclusion of the appropriate Gibbs energy corrections.

In **section 2** it was shown that the one–electron oxidation of cytosine with the loss of the electron and proton in aqueous solution (i.e. C → $e^-_{(aq)}$ + $H^+_{(aq)}$ + C(–N_4)$^{\bullet}_{(aq)}$) occurs with a sizeable free energy cost of approximately 104 kcal mol^{-1} (**Table 4**). The optimized structure of the oxidized C(–N_4)$^{\bullet}_{(aq)}$ ring (not shown) is similar to that of neutral cytosine being planar with similar bond lengths, in agreement with other theoretical studies.(Cauet et al. 2006; Wetmore et al. 2000; Wetmore et al. 1998) The calculated spin densities and Mulliken charges showed that the positive charge is delocalized over the ring with the greatest change in partial charges occurring at C_5 (+0.24e) while for spin densities they occur at C_5 (0.64) and N_1 (0.30).

The loss of a proton from N_4 in C$^{\bullet+}$ can result in the formation of either *syn*– or *anti*–C(N_4–H)$^{\bullet}$ with the former being slightly more stable (**Table 4**). However, in the resulting *anti*–form it was found that when H_2O is added, analogous to spontaneous deamination of the

neutral base,(Labet et al. 2008a) it forms a hydrogen-bond bridge between N_3 and N_4 (**RC**: **Figure 6**). Thus, only the *anti*– form is discussed herein. It is noted that the addition of H_2O has negligible effect on the Mulliken charges and spin densities of *anti*–C(N_4–H)• and with no delocalization onto the water itself.

Deamination is then initiated by transfer of a H• from the water onto the N_3 ring centre (**Figure 6**). This process proceeds via **TS1** with a barrier of 16.8 kcal mol^{-1} to give intermediate **I1**, lying 11.5 kcal mol^{-1} higher in free energy than **RC** and is thus endergonic. Intermediate **I1** resembles a complex between a cytosine tautomer and a hydroxyl radical. Interestingly, upon H• transfer the partial charge on C_4 has increased by +0.29e to 0.38e close to that observed on C_4 (0.37e) in neutral cytosine. Thus, in **I1** C_4 has the same electrophilicity as in the neutral base. Indeed, the next step is nucleophilic attack of the •OH moiety at the C_4 centre. This occurs via **TS2** with a barrier of 8.6 kcal mol^{-1} relative to **I1**; 20.1 kcal mol^{-1} with respect to **RC**. It should be noted that for spontaneous deamination of cytosine in water the analogous hydroxylation also occurs via attack of water at the C_4 position with simultaneous transfer of a proton from the H_2O moiety onto the amino N_4 centre with concomitant cleavage of the $C_4—N_4$ bond. However, it proceeds with a barrier four to five times larger than that observed above for reaction via **TS2**.(Labet et al. 2008b) In the resulting intermediate **I2**, lying just 4.2 kcal mol^{-1} higher in energy than the initial complex **RC**, the C_4 centre is now tetrahedral with a $C_4—OH$ bond length of 1.432 Å. There are then five possible pathways by which deamination of **I2** may occur, hereafter referred to as **Path A**, **B**, **C**, **D**, and **E**. The free energy changes associated with each are summarized in **Table 7**.

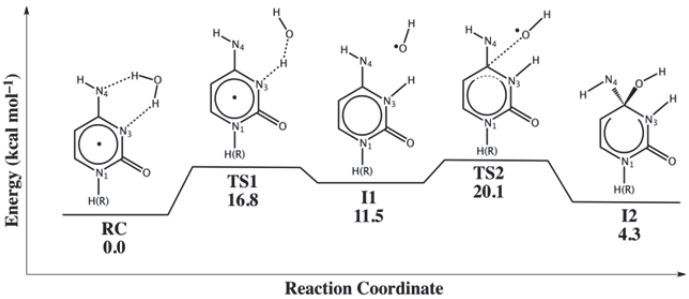

Fig. 6. Calculated (see text) relative free energies for initial abstraction of H• from H_2O by *anti*–C(N_4–H)• with subsequent attack of •OH at the C_4 centre.

Path A	ΔG	Path B	ΔG	Path C	ΔG	Path D	ΔG	Path E	ΔG
I2	4.3	**I2**	4.3	**I2**	4.3	**I2**	4.3	**I2**	4.3
^{A}**I3**	–9.0	^{B}**TS3**	38.3	^{A}**I3**	–9.0	^{D}**TS3**	31.1	^{A}**I3**	–9.0
^{A}**I4**	–0.2	^{B}**I3**	13.1	^{C}**TS3**	30.4	^{D}**I3**	6.5	^{E}**TS3**	24.9
^{A}**TS3**	7.1	^{B}**I4**	7.5	^{B}**I4**	7.5	^{D}**I4**	0.1	^{D}**I4**	0.1
^{A}**P**	–7.5	^{B}**TS4**	9.4	^{B}**TS4**	9.4	^{D}**TS4**	2.2	^{D}**TS4**	2.2
		^{B}**P**	11.4	^{B}**P**	11.4	^{D}**P**	–22.0	^{D}**P**	–22.0

Table 7. Calculated (see text) relative free energies for stationary points along **Path A**, **B**, **C**, **D** and **E** for deamination of **I2** in aqueous solution.

Path A begins with protonation of the N_4 centre in **I2** where the proton originates from the surrounding dilute aqueous solvent. The resulting intermediate ^{A}**I3** lies 13.3 kcal mol^{-1} lower in energy than **I2**. This is followed by a second protonation of N_4 with the proton again originating from the surrounding dilute aqueous solvent. In contrast to the first, this second protonation is endergonic by 8.8 kcal mol^{-1}. However, the resulting intermediate ^{A}**I4** still lies lower in energy than **I2** by 4.5 kcal mol^{-1}. In ^{A}**I4** the initial –N_4H group in **I2** has now formally become an –$N_4H_3^+$ group. Consequently, the next step is the loss of NH_3 by simple cleavage of the C—N bond. This occurs with a barrier of 7.3 kcal mol^{-1} relative to ^{A}**I4** (**Table 7**). It should be noted that the resulting product complex of ^{A}**P** lies 11.8 kcal mol^{-1} lower in energy than **I2** and resembles a complex between $NH_3^{\bullet+}$ and protonated uracil.(Labet et al. 2008b)

In contrast, in **Path B** the initial 'protonation' of N_4 is achieved via an intramolecular rearrangement from the N_3—H group and does not originate from solution. This reaction proceeds via the four-membered ring TS ^{B}**TS3** at a significant cost of 34.0 kcal mol^{-1} to give intermediate ^{B}**I3**, lying 8.8 kcal mol^{-1} higher in energy than **I2** (**Table 7**). However, similar to **Path A** the second step is protonation of N_4 with the proton originating from solution. This process is exergonic with the resulting intermediate ^{B}**I4** lying 5.6 kcal mol^{-1} lower in free energy than ^{B}**I3**. The subsequent cleavage of the C_4—$N_4H_3^+$ bond occurs via ^{B}**TS4** to give the product complex ^{B}**P**. However, unlike for **Path A**, ^{B}**P** is higher in energy than **I2** by 7.1 kcal mol^{-1} and instead resembles a complex between NH_3 and the oxidized enol form of Uracil.

Like **Path A**, the alternate **Path C** begins with the exothermic protonation of N_4 by a proton originating from solution to give ^{A}**I3** (**Table 7**). Now, however, the second proton is obtained via the intramolecular proton transfer that initiated **Path B**, i.e., by transfer from the N_3—H group. This reaction proceeds via ^{C}**TS3** with a considerable barrier of 39.4 kcal mol^{-1}, even higher than that observed in **Path B**, to give intermediate ^{B}**I4**. The remaining step, cleavage of the C_4—N_4 bond, is then identical to that of **Path B** as is the product formed.

Path D, unlike the previous paths, involves an initial intramolecular proton transfer from the C_4—OH hydroxyl onto the N_4 centre (**Table 7**). This reaction proceeds via ^{D}**TS3** at a cost of 26.8 kcal mol^{-1}. While this barrier is still quite high, it is 7.2 and 12.6 kcal mol^{-1} lower than the analogous intramolecular rearrangements in **Paths B** and **C** and is thus kinetically favoured. The resulting intermediate formed ^{D}**I3** lies only 2.2 kcal mol^{-1} higher in energy than **I2**. This is then followed by protonation of the N_4 centre by a proton originating from solution, similar to **Paths A** and **B**. This step is exothermic with the intermediate formed, ^{D}**I4**, lying 6.4 kcal mol^{-1} lower in energy than ^{D}**I3**. The next and final step is the loss of NH_3 and occurs via ^{D}**TS4** with a quite small barrier of just 2.1 kcal mol^{-1}. The resulting product ^{D}**P**, resembling a complex between NH_3 and oxidized uracil, is markedly lower in energy than **I2** by 26.3 kcal mol^{-1}. Importantly, it is in fact the lowest energy product complex obtained of all those considered herein.

The final path considered, **Path E**, begins with the same exothermic intermolecular protonation of N_4 as in **Paths A** and **C** and again leads to formation of ^{A}**I3**. The next step, however, is intramolecular proton transfer from the C_4—OH group to N_4 as occurs in **Path D**. Importantly, it proceeds via ^{E}**TS3** with a higher barrier (33.9 kcal mol^{-1}) than observed in **Path D** (26.8 kcal mol^{-1}) to give ^{D}**I4**. The final step is then cleavage of the C_4—N_4 bond as in **Path D** to give ^{D}**P**.

Thus, while deamination via donation of both protons from the aqueous solution (**Path A**) may have the lowest associated barriers, the resulting product is not the most

thermodynamically favoured. In contrast, in those cases in which only one proton originates from solution (**Paths B – E**), only those involving intramolecular rearrangement of a proton from C_4—OH (**Paths D** and **E**) are exothermic and lead to formation of the most thermodynamically preferred product (^{D}**P**). Furthermore, the barrier for this rearrangement is lowest when it occurs prior to proton donation from the solvent. Lastly in the case where both protonations occur via intermolecular processes, $NH_3^{\bullet+}$ is formed (^{A}**P**) while NH_3 is formed when only a single proton originates from exogenous sources (^{B}**P** and ^{D}**P**).

5. Oxidation of serine phosphate: Implications for DNA

As mentioned in **section 2**, the exposure of DNA to high–energy radiation can also cause damage at its phosphate backbone. In particular, it can cause strand breaks via cleavage of the phosphoester bonds.(Lipfert et al. 2004) When the absorption of radiation causes the ionization of the phosphate it has been shown that it then abstracts a $H^{\bullet}$ from the deoxyribose ring at either its $C_{4'}$ or $C_{5'}$ position. This is then followed by heterolytic cleavage of the phosphoester bond.(Lipfert et al. 2004; Steenken & Goldbergerova 1998) Alternatively, the strand break may be preceded by chemical modification of the nucleobase or deoxyribose ring or the phosphoester bond may simply undergo a direct cleavage.(Lipfert et al. 2004)

Experimentally it can be difficult to clearly observe and characterize damage within DNA due to its size. Thus, it is common to either use short fragments or model compounds that can reproduce or mimic the damage and associated processes that may occur. For example, serine phosphate contains a phosphate bond as well as a carboxylate that can act as an electron scavenger much like the bases within DNA itself. Thus, it is often used in experimental studies on the processes of DNA damage at its phosphate and subsequent bond cleavage reactions and in fact has led to a deeper understanding of those processes involved.

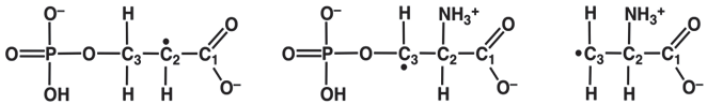

(**I**) (**II**) (**III**)

Fig. 7. The C_2-centered radical **I** and C_3-centered radicals **II** and **III** proposed to be formed upon the irradiation of non– and partially-deuterated single crystals of L–*O*–serine phosphate. (Sanderud & Sagstuen 1996)

In particular, evidence has been obtained suggesting the formation of several different radical species. Specifically, the irradiation of non– and partially-deuterated single crystals of L–*O*–serine phosphate has been suggested to produce the three radicals **I, II** and **III** shown in **Figure 7**.(Sanderud & Sagstuen 1996) In particular, it is thought that upon irradiation serine phosphate can take up a now free electron to form a C_1-centered radical anion. This may then undergo deamination to form the C_2-centered radical anion **I**. Alternatively, a serine phosphate may lose an electron to form a neutral C_1-centered radical which then undergoes decarboxylation to give a C_2-centered radical. This latter radical may then abstract a $H^{\bullet}$ from the C_3 position of another serine phosphate to generate the C_3-centered radical anion **II**. In contrast, the neutral C_3-centered radical **III** is proposed to be

formed via the uptake of a free electron by serine phosphate to give a P-centered radical anion which then simply undergoes loss of the phosphate group.

We investigated the nature of radicals **I**, **II** and **III** by obtaining optimized structures at the B3LYP/6–31G(d) level of theory. Hyperfine coupling constants (HFCCs) were then calculated via single point calculations at the B3LYP/6–311+G(2df,p) level of theory on the above structures and are listed for all three radicals in **Table 8**.(Lipfert et al. 2004)

In the optimized structure of radical **I** the largest spin density is located on C_2 (0.71) while the carbonylic oxygen of the carboxylate group also has significant spin density (0.18). This delocalization of spin density is due to conjugation between the singly occupied molecular orbital (SOMO) on C_2 and the C_1=O π–bond. In addition, it is noted that near planarity was observed for C_1 and C_2 and their substituents, in agreement with experiment.(Sanderud & Sagstuen 1996) With respect to its calculated HFCCs, as can be seen in **Table 8** the values calculated for the α–hydrogen are in good agreement with experiment. The slight deviation in A_{iso} from experiment is possibly due to the fact that the calculations are performed in the gas-phase on an isolated molecule and hence effects due to crystal packing are ignored. The calculated HFCCs for the two β–hydrogens are also in good agreement with the experiment. However, a rotational scan was performed in order to obtain the dihedral angle between the β–hydrogens and SOMO that gave HFCCs in best agreement between theory and experiment. It was found that this occurred for dihedral angles of –1.7° and 117.2°.

Radical	Atom	A_{iso}	T_{xx}	T_{yy}	T_{zz}
I	α–$H_{(calcd)}$	–43.1	28.2	–1.2	–29.5
	α–$H_{(exp)}$	–54.2	32.3	3.3	–29.0
	β–$H1_{(calcd)}$	105.6	8.7	–2.4	–6.3
	β–$H1_{(exp)}$	104.3	7.2	–2.0	–5.3
	β–$H2_{(calcd)}$	57.8	8.3	–3.6	–4.7
	β–$H2_{(exp)}$	57.4	8.1	–3.9	–4.2
II	α–$H_{(calcd)}$	–53.3	–36.1	–1.4	37.5
	α–$H_{(exp)}$	–51.0	–34.5	3.8	30.7
	β–$H_{(calcd)}$	15.4	10.8	–4.0	–6.8
	β–$H_{(exp)}$	25.0	14.0	–7.0	–8.0
	β–$N_{(calcd)}$	12.7	2.1	–0.9	–1.2
	β–$N_{(exp)}$	15.9	2.1	–0.3	–1.8
	γ–$H_{(calcd)}$	1.9	4.3	–1.5	–2.8
	γ–$H_{(exp)}$	5.9	10.1	–4.1	–5.8
III	α–$H1_{(calcd)}$	–48.8	–37.3	–1.7	39.0
	α–$H1_{(exp)}$	–47.1	–22.0	–1.5	23.6
	α–$H2_{(calcd)}$	–59.3	–37.4	–1.5	38.8
	α–$H2_{(exp)}$	–50.8	–24.6	0.5	24.2
	β–$H_{(calcd)}$	73.0	8.9	–2.2	–6.7
	β–$H_{(exp)}$	73.0	(13.3)	(–6.6)	(–6.6)

Table 8. Comparison of calculated (see text) and experimental (Sanderud & Sagstuen 1996) isotropic and anisotropic components (MHz) of the hyperfine coupling tensor of radicals **I**, **II**, and **III**.

In contrast to radical **I**, the best agreement between computational and experimental HFCCs for radicals **II** and **III** was not obtained for their proposed structures shown in **Figure 7**. Rather, the structures that gave best agreement were found to be the radical-cationic forms of **II** and **III**; that is, structures in which their phosphate and carboxylic acid groups are neutral while the amino group is protonated. Hence, these latter structures were used in all HFCC studies on radicals **II** and **III**.

For radical-cationic **II** the calculated HFCCs for the α–hydrogen are generally in good agreement with the experimental values with A_{iso} differing by just 2.3 MHz (**Table 8**). However, for both β–hydrogens, less satisfactory agreement between theory and experiment is observed. Specifically, the calculated A_{iso} values of 15.4 and 12.7 MHz differ from their corresponding experimental values by 9.6 and 3.2 MHz, respectively. As noted for the α–hydrogen in **I**, these differences are likely due to bulk crystal effects not being modeled in the calculations. Similarly, for the γ–hydrogens on the amino group, a difference of 4.0 MHz is seen between the calculated and experimental values. However, it has been stated that the given experimental value is associated with a degree of uncertainty.(Sanderud & Sagstuen 1996) In the optimized structure of **II** the C_3 centre is not completely planar where an angle between the hydrogen on C_3 and the plane defined by C_3–C_2–O was found to be 22.0°.(Lipfert et al. 2004) This is in good agreement with the corresponding experimentally determined value of 19.5°.(Sanderud & Sagstuen 1996) It is noted that the C_3 centre and adjacent oxygen have spin densities of 0.84 and 0.11 respectively, suggesting slight delocalization of the SOMO. Dobbs et al.(Dobbs et al. 1971; Dobbs et al. 1972) have suggested that this is due to incomplete rehybridization of the carbon–centered radical and is common when the carbon is bonded to an oxygen.

Indeed, in radical-cationic **III** in which the phosphate group on C_3 has been lost, i.e., there is no C_3—O bond, the radical is now fully localized on C_3. Furthermore, from **Table 8** it can be seen that quite good agreement is obtained for α-H_1 and the β-hydrogen with differences of 1.7 and 0.0 MHz respectively, while α-H_2 differs slightly more by 8.5 MHz. It should be noted that in order to obtain the best agreement for the HFCCs of the α–hydrogens they had to be tilted out of the plane by 5°. That is, the planarity of the C_3 centre had to be reduced. This is similar to that observed need in related studies on the methyl radical ($^{\bullet}CH_3$) to slightly pyramidalize the carbon centre in order to obtain best agreement between the calculated and experimentally measured HFCCs.(Eriksson et al. 1994)

6. Oxidative repair of alkylated nucleobases: the catalytic mechanism of AlkB

A common type of DNA damage is the alkylation of nucleobases at one or more of their oxygen and nitrogen centres.(Liu et al. 2009) This can be caused by endo– or exogenous agents such as S-adenosylmethionine or tobacco smoke, respectively.(Hecht 1999; Rydberg & Lindahl 1982) Consequently, cells have developed several methods by which to mediate or repair such damage. One approach is to use enzymes known as DNA glycolsylases to simply excise the damaged nucleobase via an acid-base cleavage of its N-glycosidic bond.(Mishina et al. 2006; Sedgwick et al. 2007) Alternatively, repair enzymes may use a non-redox mechanism to remove only the alkyl group. For example, O^6–methylguanine–DNA methyltransferase transfers the methyl of O^6–methylguanine onto an active site cysteinyl residue.(Lindahl et al. 1988) However, a third approach is alkyl group removal using a redox mechanism catalysed by the AlkB family of enzymes.

Although included in the α–ketoglutarate–Fe(II)–dependant dioxygenase superfamily, the AlkB family is the only one known to oxidatively dealkylate nucleobases.(Falnes et al. 2002; Trewick et al. 2002) Specifically, under physiological conditions they oxidatively repair the methylated nucleobases 1–meA, 1–meG, 3–meC and 3–meT (**Figure 8**).(Yang et al. 2008) It is noted, however, that they have been demonstrated to also be able to remove longer alkyl chains.(Delaney et al. 2005; Duncan et al. 2002; Koivisto et al. 2003; Mishina et al. 2005)

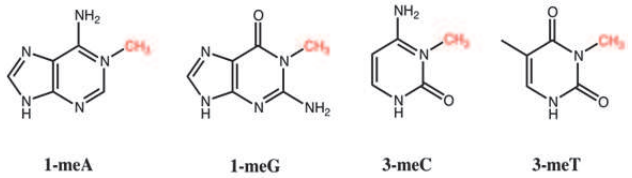

Fig. 8. Examples of methylated substrates that are dealkylated by the AlkB family of enzymes. The methyl groups to be removed have been colored in red.

Several X-ray crystal structures have been obtained of AlkB complexed with, for instance, cosubstrate or coproducts.(Yang et al. 2008; Yu et al. 2006) From these structures it was concluded that the active site of AlkB contains an Fe(II) ion ligated via two histidyl (His_{131}, His_{187}) and an aspartyl (Asp_{133}) residue. Furthermore, the α–ketoglutarate (α–KG) co-substrate bidentately ligates to the Fe(II) centre via carboxyl and ketone oxygens,(Falnes et al. 2002; Mishina et al. 2005; Trewick et al. 2002) while the methylated nucleobase sits adjacent to the Fe(II) centre. Based on these structures it was proposed that the mechanism of AlkB begins with activation of O_2: on binding to the Fe(II) centre the O_2 moiety is reduced to $O_2^{\bullet-}$ while the Fe centre is oxidized to Fe(III).(Berglund et al. 2002; Nakajima & Yamazaki 1987) The $O_2^{\bullet-}$ moiety formed then attacks the α–KG cosubstrate converting it to succinate with concomitant formation of an oxo–ferryl Fe(IV)=O species, a strong oxidizing agent.(Clifton et al. 2006; Kovaleva & Lipscomb 2008; Liu et al. 2009) However, the =O group of the oxo-ferryl sits in the apical position and thus is not ideally situated to react with the methylated nucleobase. Hence, it reorients to an equatorial position.(Yu et al. 2006)
An X-ray crystal structure (PDB: 2FD8) has been obtained under anaerobic conditions of AlkB with the single-strand trinucleotide dT-(1-me-dA)-dT bound within its active site.(Yu et al. 2006) Based on this experimental structure we obtained an appropriate chemical model for our computational studies. In particular, key active site residues, the Fe(II) centre, and α–KG modeled by pyruvate were included. A crystal structure water observed to be ligated to the Fe(II) centre in the apical position was replaced by O_2 while the substrate 1-methyladenine was modeled as 3–methyl–4–amino pyrimidinyl cation ($3me4amPym^+$). Calculations were then performed at the IEF-PCM(ε=4.0)-B3LYP/LACV3P+(d,p)//B3LYP/LACVP(d) level of theory. For complete details on the model and methods used please refer to Liu et al. 2009.(Liu et al. 2009)
In this chapter we focus on key findings of the oxidative demethylation stage of the mechanism, shown schematically in **Figure 9**. However, it should be noted that the initial O_2 activation process preferentially occurs in the quintet spin state with a rate-limiting barrier of just 9.1 kcal mol^{-1}. The lowest energy pathway for the subsequent reorientation of the Fe(IV)=O species was also found to occur for the quintet spin state. Furthermore, it was found to proceed via a concerted mechanism with a barrier of 11.3 kcal mol^{-1}. For the oxidative demethylation itself, the lowest energy pathway also occurred on the quintet

surface; the next lowest spin state, the triplet, at all times being higher in energy. Thus, herein, only the results for the quintet spin state are discussed. However, the energies for the triplet surface have been included in **Figure 9** for purposes of comparison.

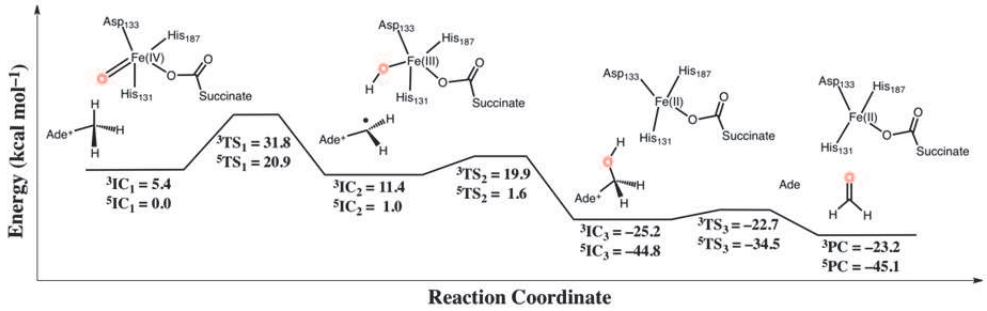

Fig. 9. Potential energy surface for the dealkylation of the methylated adenine nucleobase model 3me4amPym$^+$ in the triplet and quintet spin states.

In the apical position, the Fe(IV)=O oxygen is approximately 4.12 Å from the nearest target methyl hydrogen of the 3me4amPym$^+$ substrate. However, in ^{5}**IC$_1$**, where it now lies in the equatorial position trans to His$_{187}$, this distance has been reduced dramatically to 2.68 Å. Demethylation is initiated by abstraction of a hydrogen (H$^\bullet$) from the target methyl group of the substrate by the Fe(IV)=O oxygen. This step proceeds via the transition structure ^{5}**TS$_1$** at a cost of 20.9 kcal mol^{-1} to give intermediate ^{5}**IC$_2$** lying just 1.0 kcal mol^{-1} higher in energy than ^{5}**IC$_1$**. In ^{5}**TS$_1$** the cleaving -CH$_2$—H bond has lengthened to 1.30 Å while the corresponding FeO···H$^\bullet$ distance is quite short at 1.22 Å.(Liu et al. 2009)

This step is not only the rate limiting step in the actual demethylation of 3me4amPym$^+$, but is also the highest reaction barrier obtained in the overall mechanism of AlkB.(Liu et al. 2009) In the related α–KG–Fe(II) non–heme enzyme TauD, which catalyses hydroxylation of propene, abstraction of a methyl hydrogen by the Fe(IV)=O species was also calculated to be the rate limiting step.(de Visser 2006) The barrier in AlkB, however, is significantly higher. It has been observed that in C—H activating heme enzymes the barrier for such an abstraction is linearly related to the BDE of the substrates C—H bond being cleaved.(de Visser et al. 2004; Kaizer et al. 2004) Thus, the significantly higher barrier observed in AlkB compared to TauD is likely due to the 14.3 kcal mol^{-1} greater –CH$_2$—H bond energy in its substrate, 3me4amPym$^+$. It should be noted that experimentally k_{cat} for AlkB has been measured to be 4.5 min^{-1},(Koivisto et al. 2003; Yu et al. 2006) corresponding to a rate–limiting barrier of 19.8 kcal mol^{-1}; in good agreement with the present calculated barrier height for ^{5}**TS$_1$**.

In ^{5}**IC$_2$** the Fe(IV)=O has been reduced to Fe(III)—OH while the substrate now contains a methylene-carbon centered radical (see **Figure 9**). The next step is a 'rebound', transfer, of the hydroxyl group from the Fe–OH moiety to the substrate's radical centre. This reaction is almost barrierless proceeding via ^{5}**TS$_2$** with a cost of only 0.6 kcal mol^{-1}. Significantly, the resulting intermediate ^{5}**IC$_3$** lies markedly lower in energy than ^{5}**IC$_1$** by –44.8 kcal mol^{-1}. Thus, effectively, the result of the first two steps in demethylation are exothermic insertion of an oxygen into a C—H bond of the substrates methyl group with reduction of the Fe(IV) centre to Fe(II). The much lower relative energy of ^{5}**IC$_3$** may also reflect the structural rearrangement that occurs at the Fe centre which has gone from penta– to tetra-coordinate.

The final step in the demethylation of 3me4amPym$^+$ is decomposition of the hydroxylated intermediate to give 4–amino pyrimidine, the model for the demethylated nucleobase, and formaldehyde (**Figure 9**). In this step an active site Glu_{136} residue acts as a general base and deprotonates the Ade–CH_2OH hydroxyl with concomitant cleavage of the $_{Ade}N-CH_2OH$ bond.(Liu et al. 2009) This reaction proceeds via ^{5}**TS$_3$** at the modest cost of 10.3 kcal mol^{-1}. It is noted that in ^{5}**TS$_3$** the $_{Ade}N\cdots CH_2OH$ and Ade-CH_2O-H bonds have lengthened to 1.58 and 1.22 Å, respectively, highlighting their concomitant cleavage. The product-bound complex ^{5}**PC** lies 45.1 kcal mol^{-1} lower in relative energy than the initial reactant complex ^{5}**IC$_1$**. Thus, demethylation of 1-methyladenine is calculated to be a quite exothermic process.

7. Conclusion

In this chapter the application of density functional theory (DFT)-based methods to the study of DNA damage and repair mechanisms has been illustrated.

In particular, it was shown how they may be used to provide accurate detailed insights into the thermochemistry of fundamental chemical processes such as electron and proton transfers and thus, help to explain a number of experimental observations. Furthermore, through such studies they were able to show differences in the preferred oxidation pathways for the various DNA nucleobases. Similarly, by the careful examination of calculated hyperfine coupling constants, the nature *and* structure of radicals that may be formed upon exposure of DNA to radiation were deduced. Such an understanding also aids in determining the mechanism by which they may be formed. Finally, their versatility for the investigation of damage and repair mechanisms was highlighted. Indeed, by examining several pathways using seemingly quite simple chemical models, we have been able to deduce the preferred mechanism by which the deamination of cytosine radical may occur including (i) the preferred proton source(s), (ii) the order in which they are added to the leaving nitrogen centre, and (iii) the thermodynamically preferred products. Finally, similar methods in combination with much larger chemical models were used to also elucidate the oxidative dealkylation repair mechanism of AlkB. Together, these studies highlight the versatility and accuracy of DFT methods when used in combination with well-chosen chemical models for the study of DNA damage and repair.

8. Acknowledgements

JWG, JL and EACB acknowledge the Natural Sciences and Engineering Research Council (NSERC, Canada) for funding and CGS & PGSD scholarships (EACB) and JL and LAE thank the Swedish Science Research Council (VR) for funding. LAE also acknowledges the National University of Ireland (Galway) for financial support. SHARCNET (Canada) and the National Supercomputing Centre (Linköping, Sweden) are acknowledged for additional computational resources.

9. References

Almatarneh, M. H., Flinn, C. G., Poirier, R. A., & Sokalski, W. A. (2006). "Computational study of the deamination reaction of cytosine with H_2O and OH." *J. Phys. Chem. A*, 110(26), 8227-8234.

Becke, A. D. (1993a). "A Mixing of Hartree-Fock and Local Density-Functional Theories." *J. Chem. Phys.*, 98, 1372.

Becke, A. D. (1993b). "Density-Functional Thermochemistry .3. The Role of Exact Exchange." *J. Chem. Phys.*, 98(7), 5648-5652.

Berglund, G. I., Carlsson, G. H., Smith, A. T., Szoke, H., Henriksen, A., & Hajdu, J. (2002). "The catalytic pathway of horseradish peroxidase at high resolution." *Nature*, 417(6887), 463-468.

Burrows, C. J., & Muller, J. G. (1998). "Oxidative nucleobase modifications leading to strand scission." *Chem. Rev.*, 98(3), 1109-1151.

Cadet, J., Douki, T., & Ravanat, J. L. (2006). "One-electron oxidation of DNA and inflammation processes." *Nat. Chem. Biol.*, 2(7), 348-349.

Cadet, J., Douki, T., & Ravanat, J. L. (2008). "Oxidatively generated damage to the guanine moiety of DNA: Mechanistic aspects and formation in cells." *Accounts Chem. Res.*, 41(8), 1075-1083.

Cadet, J., & Vigny, P. (1990). Bioorganic Photochemistry. Photochemistry and the Nucleic Acids, H. Morrison, ed., Wiley, New York, 1-272.

Cammi, R., & Tomasi, J. (1995). "Remarks on the use of the apparent surface-charges (ASC) methods in solvation problems - Iterative versus matrix-inversion procedures and the renormalization of the apparent charges." *J. Comput. Chem.*, 16(12), 1449-1458.

Cances, E., & Mennucci, B. (1998). "New applications of integral equations methods for solvation continuum models: ionic solutions and liquid crystals." *J. Math. Chem.*, 23(3-4), 309-326.

Cances, E., Mennucci, B., & Tomasi, J. (1997). "A new integral equation formalism for the polarizable continuum model: Theoretical background and applications to isotropic and anisotropic dielectrics." *J. Chem. Phys.*, 107(8), 3032-3041.

Candeias, L. P., & Steenken, S. (2000). "Reaction of HO center dot with guanine derivatives in aqueous solution: Formation of two different redox-active OH-Adduct radicals and their unimolecular transformation reactions. Properties of G(-H)(center dot)." *Chem.-Eur. J.*, 6(3), 475-484.

Cauet, E., Dehareng, D., & Lievin, J. (2006). "Ab initio study of the ionization of the DNA bases: Ionization potentials and excited states of the cations." *J. Phys. Chem. A*, 110(29), 9200-9211.

Chatgilialoglu, C., Ferreri, C., Bazzanini, R., Guerra, M., Choi, S. Y., Emanuel, C. J., Horner, J. H., & Newcomb, M. (2000). "Models of DNA C1 ' radicals. Structural, spectral, and chemical properties of the thyminylmethyl radical and the 2 '-deoxyuridin-1 '-yl radical." *J. Am. Chem. Soc.*, 122(39), 9525-9533.

Cheng, K. C., Cahill, D. S., Kasai, H., Nishimura, S., & Loeb, L. A. (1992). "8-hydroxyguanine, an abundant form of oxidative dna damage, causes g -> t and a -> c substitutions." *J. Biol. Chem.*, 267(1), 166-172.

Clifton, I. J., McDonough, M. A., Ehrismann, D., Kershaw, N. J., Granatino, N., & Schofield, C. J. (2006). "Structural studies on 2-oxoglutarate oxygenases and related double-stranded beta-helix fold proteins." *J. Inorg. Biochem.*, 100(4), 644-669.

Cullis, P. M., Malone, M. E., & MersonDavies, L. A. (1996). "Guanine radical cations are precursors of 7,8-dihydro-8-oxo-2'-deoxyguanosine but are not precursors of immediate strand breaks in DNA." *J. Am. Chem. Soc.*, 118(12), 2775-2781.

De Bont, R., & van Larebeke, N. (2004). "Endogenous DNA damage in humans: a review of quantitative data." *Mutagenesis*, 19(3), 169-185.

de Visser, S. P. (2006). "Propene activation by the oxo-iron active species of taurine/alpha-ketoglutarate dioxygenase (TauD) enzyme. How does the catalysis compare to heme-enzymes?" *J. Am. Chem. Soc.*, 128(30), 9813-9824.

de Visser, S. P., Kumar, D., Cohen, S., Shacham, R., & Shaik, S. (2004). "A predictive pattern of computed barriers for C-H hydroxylation by compound I of cytochrome P450." *J. Am. Chem. Soc.*, 126(27), 8362-8363.

Decarroz, C., Wagner, J. R., & Cadet, J. (1987). *Free Radical Res. Commun.*(2), 295-301.

Decarroz, C., Wagner, J. R., Vanlier, J. E., Krishna, C. M., Riesz, P., & Cadet, J. (1986). "Sensitized photooxidation of thymidine by 2-methyl-1-1,4-naphthoquinone - characterization of the stable photoproducts." *Int. J. Radiat. Biol.*, 50(3), 491-505.

Delaney, J. C., Smeester, L., Wong, C. Y., Frick, L. E., Taghizadeh, K., Wishnok, J. S., Drennan, C. L., Samson, L. D., & Essigmann, J. M. (2005). "AlkB reverses etheno DNA lesions caused by lipid oxidation in vitro and in vivo." *Nat. Struct. Mol. Biol.*, 12(10), 855-860.

Dobbs, A. J., Gilbert, B. C., & Norman, R. O. C. (1971). "Electron spin resonance studies .27. geometry of oxygen-substituted alkyl radicals." *J. Chem. Soc. A*(1), 124-&.

Dobbs, A. J., Gilbert, B. C., & Norman, R. O. C. (1972). "Electron-spin resonance studies .32. information from hyperfine splittings for aliphatic radicals about shape and conformation." *J. Chem. Soc.-Perkin Trans. 2*(6), 786-&.

Douki, T., & Cadet, J. (1999). "Modification of DNA bases by photosensitized one-electron oxidation." *Int. J. Radiat. Biol.*, 75(5), 571-581.

Duncan, T., Trewick, S. C., Koivisto, P., Bates, P. A., Lindahl, T., & Sedgwick, B. (2002). "Reversal of DNA alkylation damage by two human dioxygenases." *Proc. Natl. Acad. Sci. U. S. A.*, 99(26), 16660-16665.

Eley, D. D., & Spivey, D. I. (1962). "Semiconductivity of organic substances .9. Nucleic acid in dry state." *Trans. Faraday Soc.*, 58, 411.

Eriksson, L. A., Malkin, V. G., Malkina, O. L., & Salahub, D. R. (1994). "The effects of nonlocal gradient corrections in density-functional calculations of hydrocarbon radical hyperfine structures." *Int. J. Quantum Chem.*, 52(4), 879-901.

Falnes, P. O., Johansen, R. F., & Seeberg, E. (2002). "AlkB-mediated oxidative demethylation reverses DNA damage in Escherichia coli." *Nature*, 419(6903), 178-182.

Friedberg, E. C., McDaniel, L. D., & Schultz, R. A. (2004). "The role of endogenous and exogenous DNA damage and mutagenesis." *Curr. Opin. Genet. Dev.*, 14(1), 5-10.

Hagen, U. (1986). "Current aspects on the radiation-induced base damage in dna." *Radiat. Environ. Biophys.*, 25(4), 261-271.

Hatahet, A., & Wallace, Z.Z. (1998). DNA Damage and Repair, DNA Repair in Prokaryotes and Lower Eukaryotes, J. A. Nickoloff, Hoekstra, M.F., ed., Humana Press, New Jersey.

Hecht, S. S. (1999). "DNA adduct formation from tobacco-specific N-nitrosamines." *Mutat. Res.-Fundam. Mol. Mech. Mutagen.*, 424(1-2), 127-142.

Hush, N. S., & Cheung, A. S. (1975). "Ionization-potentials and donor properties of nucleic-acid bases and related compounds." *Chem. Phys. Lett.*, 34(1), 11-13.

Kaizer, J., Klinker, E. J., Oh, N. Y., Rohde, J. U., Song, W. J., Stubna, A., Kim, J., Munck, E., Nam, W., & Que, L. (2004). "Nonheme (FeO)-O-IV complexes that can oxidize the C-H bonds of cyclohexane at room temperature." *J. Am. Chem. Soc.*, 126(2), 472-473.

Kamiya, H., Iwai, S., & Kasai, H. (1998). "The (6-4) photoproduct of thymine-thymine induces targeted substitution mutations in mammalian cells." *Nucleic Acids Res.*, 26(11), 2611-2617.

Kasai, H., Crain, P. F., Kuchino, Y., Nishimura, S., Ootsuyama, A., & Tanooka, H. (1986). "Formation of 8-hydroxyguanine moiety in cellular dna by agents producing oxygen radicals and evidence for its repair." *Carcinogenesis*, 7(11), 1849-1851.

Koivisto, P., Duncan, T., Lindahl, T., & Sedgwick, B. (2003). "Minimal methylated substrate and extended substrate range of Escherichia coli AlkB protein, a 1-methyladenine-DNA dioxygenase." *J. Biol. Chem.*, 278(45), 44348-44354.

Kovaleva, E. G., & Lipscomb, J. D. (2008). "Versatility of biological non-heme Fe(II) centers in oxygen activation reactions." *Nat. Chem. Biol.*, 4(3), 186-193.

Kumar, A., & Sevilla, M. D. (2010). "Proton-Coupled Electron Transfer in DNA on Formation of Radiation-Produced Ion Radicals." *Chem. Rev.*, 110(12), 7002-7023.

Labet, V., Grand, A., Cadet, J., & Eriksson, L. A. (2008a). "Deamination of the radical cation of the base moiety of 2 '-deoxycytidine: A theoretical study." *ChemPhysChem*, 9(8), 1195-1203.

Labet, V., Grand, A., Morell, C., Cadet, J., & Eriksson, L. A. (2008b). "Proton catalyzed hydrolytic deamination of cytosine: a computational study." *Theor. Chem. Acc.*, 120(4-6), 429-435.

Labet, V., Grand, A., Morell, C., Cadet, J., & Eriksson, L. A. (2009). "Mechanism of nitric oxide induced deamination of cytosine." *Phys. Chem. Chem. Phys.*, 11, 2379-2386.

Lee, C. T., Yang, W. T., & Parr, R. G. (1988). "Development of the colle-salvetti correlation-energy formula into a functional of the electron-density." *Phys. Rev. B*, 37(2), 785-789.

Lee, Y. A., Yun, B. H., Kim, S. K., Margolin, Y., Dedon, P. C., Geacintov, N. E., & Shafirovich, V. (2007). "Mechanisms of oxidation of guanine in DNA by carbonate radical anion, a decomposition product of nitrosoperoxycarbonate." *Chem.-Eur. J.*, 13(16), 4571-4581.

Lindahl, T. (1993). "Instability and decay of the primary structure of dna." *Nature*, 362(6422), 709-715.

Lindahl, T., Sedgwick, B., Sekiguchi, M., & Nakabeppu, Y. (1988). "Regulation and expression of the adaptive response to alkylating-agents." *Annu. Rev. Biochem.*, 57, 133-157.

Lipfert, J., Llano, J., & Eriksson, L. A. (2004). "Radiation-induced damage in serine phosphate-insights into a mechanism for direct DNA strand breakage." *J. Phys. Chem. B*, 108(23), 8036-8042.

Liu, H. N., Llano, J., & Gauld, J. W. (2009). "A DFT Study of Nucleobase Dealkylation by the DNA Repair Enzyme AlkB." *J. Phys. Chem. B*, 113(14), 4887-4898.

Llano, J., & Eriksson, L. A. (2002). "First principles electrochemistry: Electrons and protons reacting as independent ions." *J. Chem. Phys.*, 117(22), 10193-10206.

Llano, J., & Eriksson, L. A. (2004a). "First principles electrochemical study of redox events in DNA bases and chemical repair in aqueous solution." *Phys. Chem. Chem. Phys.*, 6(9), 2426-2433.

Llano, J., & Eriksson, L. A. (2004b). "Oxidation pathways of adenine and guanine in aqueous solution from first principles electrochemistry." *Phys. Chem. Chem. Phys.*, 6(19), 4707-4713.

Llano, J., & Gauld, J.W. (2010). Mechanistics of Enzyme Catalysis: From Small to Large Active-Site Models, In: *Quantum Biochemistry: Electronic Structure and Biological Activity*, Matta, C. F., 643-666, Wiley-VCH, Weinheim.

Lysetska, M., Knoll, A., Boehringer, D., Hey, T., Krauss, G., & Krausch, G. (2002). "UV light-damaged DNA and its interaction with human replication protein A: an atomic force microscopy study." *Nucleic Acids Res.*, 30(12), 2686-2691.

Mennucci, B., Cances, E., & Tomasi, J. (1997). "Evaluation of solvent effects in isotropic and anisotropic dielectrics and in ionic solutions with a unified integral equation method: Theoretical bases, computational implementation, and numerical applications." *J. Phys. Chem. B*, 101(49), 10506-10517.

Miertus, S., Scrocco, E., & Tomasi, J. (1981). "Electrostatic interaction of a solute with a continuum - a direct utilization of abinitio molecular potentials for the prevision of solvent effects." *Chem. Phys.*, 55(1), 117-129.

Mishina, Y., Duguid, E. M., & He, C. (2006). "Direct reversal of DNA alkylation damage." *Chem. Rev.*, 106(2), 215-232.

Mishina, Y., Yang, C. G., & He, C. (2005). "Direct repair of the exocyclic DNA adduct 1,N-6-ethenoadenine by the DNA repair AlkB proteins." *J. Am. Chem. Soc.*, 127(42), 14594-14595.

Munk, B. H., Burrows, C. J., Schlegel, H. B. (2008). "An Exploration of Mechanisms for the Transformation of 8-Oxoguanine to Guanidinohydantoin and Spiroiminodihydantoin by Density Functional Theory." *J. Am. Chem. Soc.*, 130, 5245-5256

Nakajima, R., & Yamazaki, I. (1987). "The mechanism of oxyperoxidase formation from ferryl peroxidase and hydrogen-peroxide." *J. Biol. Chem.*, 262(6), 2576-2581.

Neeley, W. L., & Essigmann, J. M. (2006). "Mechanisms of formation, genotoxicity, and mutation of guanine oxidation products." *Chem. Res. Toxicol.*, 19(4), 491-505.

Newcomb, T. G., & Loeb, L.A. (1998). DNA Damage and Repair, DNA Repair in Prokaryotes and Lower Eukaryotes, J. A. Nickoloff, Hoekstra, M.F., ed., Humana Press, New Jersey.

Pages, V., & Fuchs, R. P. P. (2002). "How DNA lesions are turned into mutations within cells?" *Oncogene*, 21(58), 8957-8966.

Pavlov, Y. I., Minnick, D. T., Izuta, S., & Kunkel, T. A. (1994). "DNA-replication fidelity with 8-oxodeoxyguanosine triphosphate." *Biochemistry*, 33(15), 4695-4701.

Rydberg, B., & Lindahl, T. (1982). "Non-enzymatic methylation of DNA by the intracellular methyl-group donor s-adenosyl-l-methionine is a potentially mutagenic reaction." *Embo J.*, 1(2), 211-216.

Sanderud, A., & Sagstuen, E. (1996). "EPR and ENDOR studies of H-1 and N-14 hyperfine and quadrupolar couplings in crystals of L-O-serine phosphate after X-irradiation at 295 K." *J. Phys. Chem.*, 100(22), 9545-9555.

Sedgwick, B., Bates, P. A., Paik, J., Jacobs, S. C., & Lindahl, T. (2007). "Repair of alkylated DNA: Recent advances." *DNA Repair*, 6(4), 429-442.

Seidel, C. A. M., Schulz, A., & Sauer, M. H. M. (1996). "Nucleobase-specific quenching of fluorescent dyes .1. Nucleobase one-electron redox potentials and their correlation with static and dynamic quenching efficiencies." *J. Phys. Chem.*, 100(13), 5541-5553.

Sponer, J. E., Miguel, P. J. S., Rodriguez-Santiago, L., Erxleben, A., Krumm, M., Sodupe, M., Sponer, J., & Lippert, B. (2004). "Metal-mediated deamination of cytosine: Experiment and DFT calculations." *Angew. Chem.-Int. Edit.*, 43(40), 5396-5399.

Steenken, S. (1989). "Purine-bases, nucleosides, and nucleotides - aqueous-solution redox chemistry and transformation reactions of their radical cations and e- and OH adducts." *Chem. Rev.*, 89(3), 503-520.

Steenken, S. (1992). "Electron-transfer-induced acidity basicity and reactivity changes of purine and pyrimidine-bases - consequences of redox processes for DNA-base pairs." *Free Radic. Res. Commun.*, 16(6), 349-379.

Steenken, S., & Goldbergerova, L. (1998). "Photoionization of organic phosphates by 193 nm laser light in aqueous solution: Rapid intramolecular H-transfer to the primarily formed phosphate radical. A model for ionization-induced chain-breakage in DNA?" *J. Am. Chem. Soc.*, 120(16), 3928-3934.

Steenken, S., & Jovanovic, S. V. (1997). "How easily oxidizable is DNA? One-electron reduction potentials of adenosine and guanosine radicals in aqueous solution." *J. Am. Chem. Soc.*, 119(3), 617-618.

Steenken, S., Telo, J. P., Novais, H. M., & Candeias, L. P. (1992). "One-electron-reduction potentials of pyrimidine-bases, nucleosides, and nucleotides in aqueous-solution - consequences for DNA redox chemistry." *J. Am. Chem. Soc.*, 114(12), 4701-4709.

Taylor, J. S. (1994). "Unraveling the molecular pathway from sunlight to skin-cancer." *Accounts Chem. Res.*, 27(3), 76-82.

Teoule, R. (1987). "Radiation-induced DNA damage and its repair." *Int. J. Radiat. Biol.*, 51(4), 573-589.

Trewick, S. C., Henshaw, T. F., Hausinger, R. P., Lindahl, T., & Sedgwick, B. (2002). "Oxidative demethylation by Escherichia coli AlkB directly reverts DNA base damage." *Nature*, 419(6903), 174-178.

von Sonntag, C. (1987). *The Chemical Basis of Radiation Biology*, Taylor & Francis, London.

von Sonntag, C., Schuchmann, H.P. (1996). Encyclopedia of Molecular Biology and Molecular Medicine, R. A. Meyers, ed., VCH, Weinheim.

Wagner, J. R., Vanlier, J. E., Decarroz, C., Berger, M., & Cadet, J. (1990). "Photodynamic methods for oxy radical-induced dna-damage." *Method Enzymol.*, 186, 502-511.

Wang, Y. S. (2008). "Bulky DNA lesions induced by reactive oxygen species." *Chem. Res. Toxicol.*, 21(2), 276-281.

Wetmore, S. D., Boyd, R. J., & Eriksson, L. A. (2000). "Electron affinities and ionization potentials of nucleotide bases." *Chem. Phys. Lett.*, 322(1-2), 129-135.

Wetmore, S. D., Eriksson, L. A. & Boyd, R. J., (2001). A Multi-Component Model for Radiation Damage to DNA from its Constituents in Theoretical Biochemistry Processes and Properties of Biological Systems, In: *Theoretical and Computational Chemistry*, Eriksson, L. A., 409-466, Elsevier, Amsterdam.

Wetmore, S. D., Himo, F., Boyd, R. J., & Eriksson, L. A. (1998). "Effects of ionizing radiation on crystalline cytosine monohydrate." *J. Phys. Chem. B*, 102(38), 7484-7491.

Yang, C. G., Yi, C. Q., Duguid, E. M., Sullivan, C. T., Jian, X., Rice, P. A., & He, C. (2008). "Crystal structures of DNA/RNA repair enzymes AlkB and ABH2 bound to dsDNA." *Nature*, 452(7190), 961-U4.

Yang, X., Wang, X. B., Vorpagel, E. R., & Wang, L. S. (2004). "Direct experimental observation of the low ionization potentials of guanine in free oligonucleotides by using photoelectron spectroscopy." *Proc. Natl. Acad. Sci. U. S. A.*, 101(51), 17588-17592.

Yao, L. S., Li, Y., Wu, Y., Liu, A. Z., & Yan, H. G. (2005). "Product release is rate-limiting in the activation of the prodrug 5-fluorocytosine by yeast cytosine deaminase." *Biochemistry*, 44(15), 5940-5947.

Yu, B., Edstrom, W. C., Benach, J., Hamuro, Y., Weber, P. C., Gibney, B. R., & Hunt, J. F. (2006). "Crystal structures of catalytic complexes of the oxidative DNA/RNA repair enzyme AlkB." *Nature*, 439(7078), 879-884.

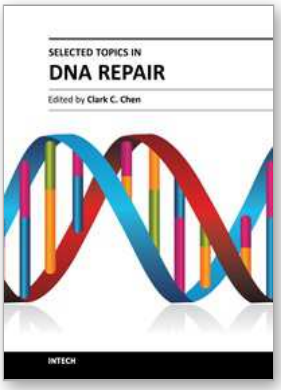

Selected Topics in DNA Repair

Edited by Prof. Clark Chen

ISBN 978-953-307-606-5
Hard cover, 572 pages
Publisher InTech
Published online 26, October, 2011
Published in print edition October, 2011

This book is intended for students and scientists working in the field of DNA repair, focusing on a number of topics ranging from DNA damaging agents and mechanistic insights to methods in DNA repair and insights into therapeutic strategies. These topics demonstrate how scientific ideas are developed, tested, dialogued, and matured as it is meant to discuss key concepts in DNA repair. The book should serve as a supplementary text in courses and seminars as well as a general reference for biologists with an interest in DNA repair.

How to reference

In order to correctly reference this scholarly work, feel free to copy and paste the following:

Eric A. C. Bushnell, Jorge Llano, Leif A. Eriksson and James W. Gauld (2011). Mechanisms of Mutagenic DNA Nucleobase Damages and Their Chemical and Enzymatic Repairs Investigated by Quantum Chemical Methods, Selected Topics in DNA Repair, Prof. Clark Chen (Ed.), ISBN: 978-953-307-606-5, InTech, Available from: http://www.intechopen.com/books/selected-topics-in-dna-repair/mechanisms-of-mutagenic-dna-nucleobase-damages-and-their-chemical-and-enzymatic-repairs-investigated

INTECH
open science | open minds

InTech Europe
University Campus STeP Ri
Slavka Krautzeka 83/A
51000 Rijeka, Croatia
Phone: +385 (51) 770 447
Fax: +385 (51) 686 166
www.intechopen.com

InTech China
Unit 405, Office Block, Hotel Equatorial Shanghai
No.65, Yan An Road (West), Shanghai, 200040, China
中国上海市延安西路65号上海国际贵都大饭店办公楼405单元
Phone: +86-21-62489820
Fax: +86-21-62489821